

# Hopping control for the musculoskeletal bipedal robot: BioBiped

Maziar A. Sharbafi, Katayon Radkhah, Oskar von Stryk and Andre Seyfarth

**Abstract**—Bipedal locomotion can be divided into primitive tasks, namely repulsive leg behavior (bouncing against gravity), leg swing (protraction and retraction) and body alignment (balancing against gravity). In the bipedal spring-mass model for walking and running, the repulsive leg function is described by a linear prismatic spring. This paper adopts two strategies for swinging and bouncing control from conceptual models for the human-inspired musculoskeletal BioBiped robot. The control approach consists of two layers, velocity based leg adjustment (VBLA) and virtual model control to represent a virtual springy leg between toe and hip. Additionally, the rest length and stiffness of the virtual springy leg are tuned based on events to compensate energy losses due to damping. In order to mimic human locomotion, the trunk is held upright by physical constraints. The controller is implemented on the validated detailed simulation model of BioBiped. In-place as well as forward hopping and switching between these two gaits are easily achieved by tuning the parameters for the leg adjustment, virtual leg stiffness and injected energy. Furthermore, it is shown that the achieved motion performance of in-place hopping agrees well with that of human subjects.

## I. INTRODUCTION

Robots can help to demonstrate and prove concepts on human locomotion such as concepts based on springlike leg behavior. Starting from simple models, hopping is a simple 1D motion which can be described with the SLIP (Spring Loaded Inverted Pendulum) model [1]. Then, a first basic mechanical function in human locomotion is rebounding on compliant legs, which can be described by a leg spring like running [2] and walking [3].

Simple conceptual models, coined “templates” [4] have proved to be very helpful for describing and analyzing legged locomotion. In that respect, developing bipedal robots based on human morphology and locomotion can be inspired by these simple models [5][6], in spite of their high level of abstraction. Another interesting property of the SLIP is its asymptotic stability against perturbations conserving energy, even with a constant angle of attack [2].

In [7], Pratt presented the Virtual Model Control (VMC) approach to create virtual forces when the virtual components interact with a robot system [8]. Due to the complexity of the robots and, of course humans, the implementation of stabilizing strategies is a challenge. However, fundamental strategies to gain stability can be deduced from very simple

models. Hence, in this paper VMC is employed to represent a virtual spring between toe and hip in order to resemble the SLIP model.

The second control level, which is needed when the motion is planar instead of 1D, is leg adjustment. Unlike running [2] and walking [3], stable hopping in 2D cannot be achieved with a fixed angle of attack with respect to the ground. So, to recover from any perturbation, a robust method to find the appropriate leg direction during the flight phase is necessary for hopping in place. In literature, the leg adjustment strategies are mostly following the Raibert approach [5] in which the foot landing position is adjusted based on the horizontal velocity (e.g. [9][10]). Recently, Peuker et al. [11] investigated different strategies and showed that applying both CoM velocity and gravity vectors result in very robust hopping and running with SLIP model. In this paper we utilized Velocity Based Leg Adjustment (VBLA) introduced in [12] which is an improved version of Peuker’s approach[11].

Further, hip springs support faster steps and accelerate swing leg motion [13][14]. The latter effect may equally be achieved by implementing elastic tendons between the upper body and the legs [15]. The compliant coupling of the upper body and legs is also existent in the human body, e.g. the Rectus femoris and Hamstring muscles (see Fig.1(a)). We also have implemented these biarticular muscles in the BioBiped robot which is our test bed for evaluating the control approaches.

From [16], it is concluded that upright trunk is a key feature for human locomotion. Because of the robot limitations, balancing is not considered in this paper. Thus, we keep the trunk upright by some constraining mechanisms. Implementing a proper posture control strategy like VPP [16] is targeted with a redesigned robot.

In this study, a controller which is designed based on template models is presented for hopping in place and forward hopping just with tuning a few parameters. This controller is applied to BioBiped, a biologically inspired, musculoskeletal bipedal robot consisting two 3-segmented legs and a rigid trunk that can tilt for- and backwards as shown in Fig. 1(c). Projection of the robot model on the conceptual model, designing the controller for the simplified model and extending it to the complex model are different steps of the proposed control approach. Energy management via event based control, leg adjustment and position control construct different parts of the controller. Similarity of the robot structure and controlled motion to humans and changing the hopping speed with leg angle adjustment and energy compensation just with tuning few parameters are the

This research was supported in part by the German Research Foundation (DFG) under grants No. SE1042/8.

M. A. Sharbafi and A. Seyfarth are with the Laufflabor Laboratory, Technische Universität Darmstadt, Darmstadt, Germany, {sharbafi, seyfarth}@sport.tu-darmstadt.de

K. Radkhah and O. von Stryk are with the Simulation, Systems Optimization and Robotics Group, Technische Universität Darmstadt, Darmstadt, Germany, {radkhah, stryk}@sim.tu-darmstadt.de

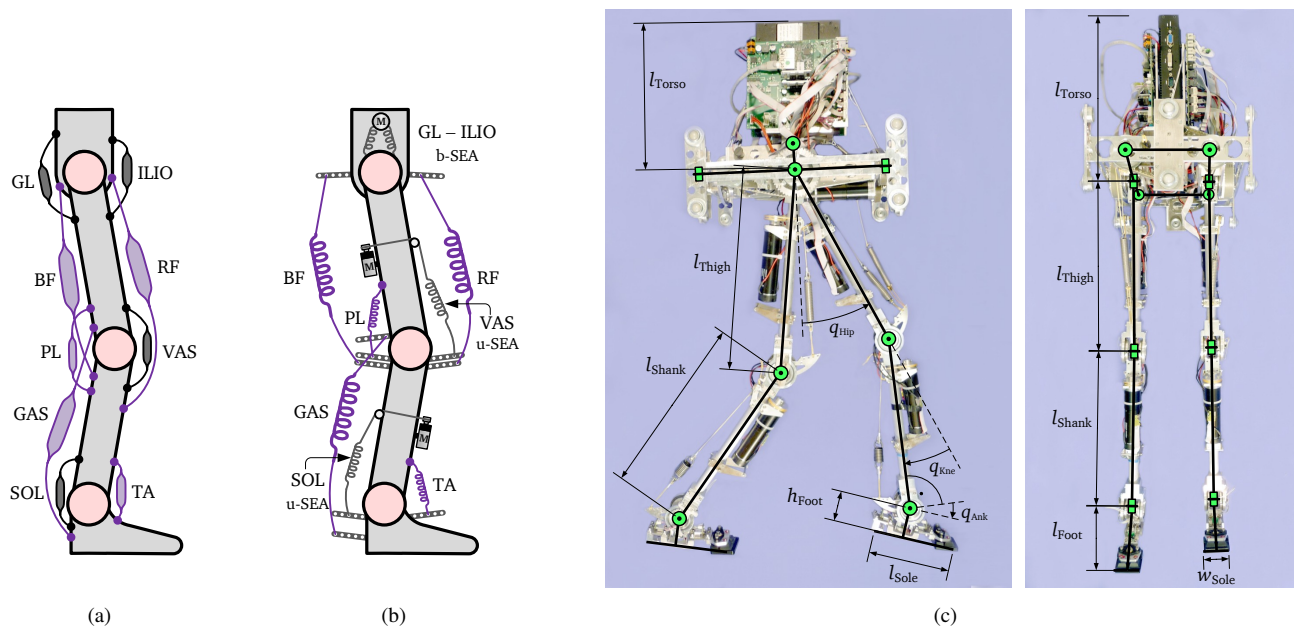


Fig. 1. Technical realization of BioBiped1 and its actuation from left to right: (a) Essential human muscle groups during locomotion: Actuated tendons are indicated by dark grey color, while passive tendons are marked in purple; (b) constructed version of BioBiped1's actuation with u-SEA and b-SEA denoting a unidirectional and bidirectional series elastic actuator, respectively [17]; (c) real robot platform with its main kinematic and dynamic parameters given in Table I. Pictures are taken from [18].

main contributions in this paper. The results from a detailed simulation model of the robot show the performance of the proposed method. The comparison with human hopping in place which help to improve the robot structure in the next generations<sup>1</sup> toward designing a controlled robot mimicking human locomotion.

## II. METHODS

### A. Simulation Model

The BioBiped1 robot, built within the BioBiped project<sup>2</sup>, represents a biologically inspired robot featuring a highly compliant actuation system [19]. It is about 1.1 m tall in extended position with the body mass of 10 kg. For the main kinematics and dynamics data we refer to Table I. Both legs have rotational degrees of freedom (DoF), one in hip, knee and ankle joint along the pitch axis.

1) *Actuation concept and its technical realization:* BioBiped's actuation is inspired by the human musculoskeletal system, in which monoarticular and biarticular muscles, i.e. muscles that span two joints, work together [19]. In Fig. 1(a) we have depicted nine muscle groups mainly acting in sagittal plane during human locomotion. The monoarticular muscles contribute to the task of power generation [20]. Each joint is coupled to a pair of monoarticular muscles: *Iliopsoas* (ILIO) - *Gluteus Maximus* (GL) in the hip, *Popliteus* (PL) - *Vastus lateralis* (VAS) in the knee and *Tibialis anterior* (TA) - *Soleus* (SOL) in the ankle for the respective flexion and extension. The biarticular muscles are known to transfer energy from proximal to distal joints and to synchronize joint

function of hip, knee and ankle [21]. The muscles *Rectus femoris* (RF) and *Biceps Femoris* (BF) cross both the hip and knee joint. While RF acts as combined knee extensor and hip flexor, BF behaves exactly the other way. The knee and ankle joints are coupled by the *Gastrocnemius* (GAS).

As for the technical realization, all the biarticular and monoarticular flexing muscles are represented as passive tendons with a built-in extension spring, i.e. they act completely passively based on the actual joint configurations and external forces. All other muscles, the pair in the hip as well as the knee and ankle extensors, are actively integrated. A bidirectional series elastic actuator connecting the hip joint to the motor via a timing belt supports actively both the flexion and extension. In the knee and ankle the geared electric motors are coupled to the joints by an elastic tendon consisting of a Dyneema tendon with built-in spring. For attaching the tendons at the joints several different attachment points are available. This leg actuation concept introduces varying lever arms and transmission ratios aside from highly nonlinear joint torques and stiffnesses.

The geared rotary electric direct-current motors were appropriately selected prior to the robot's construction using a model-based motion generation and control method [22]. For more details regarding the actuation decisions we refer to [19].

2) *Detailed physical modeling and simulation:* A detailed simulation model of the real robot was developed in order to efficiently design and test different control strategies prior to direct experimentation on the real robot. The simulation model was developed in MATLAB with Simulink and Sim-Mechanics using object-oriented design to ease the analyses and data management [23]. The multi-body system (MBS)

<sup>1</sup>Two versions of BioBipeds were already manufactured and BioBiped III is in the designing step.

<sup>2</sup>See the project page <http://www.biobiped.de>

TABLE I  
MAIN KINEMATICS AND DYNAMICS DATA OF THE BIOBIPED1 ROBOT.

Dimensions and Masses	
Segment lengths	$l_{Torso} = 269$ mm; $l_{Thigh} = 330$ mm; $l_{Shank} = 330$ mm; $l_{Foot} = 122$ mm
Foot dimensions	$h_{Foot} = 67$ mm; $l_{Sole} = 165$ mm; $w_{Sole} = 40$ mm
Leg length	0.727 m (from hip to sole with extended leg)
Segment masses	$m_{Torso} = 5.332$ kg; $m_{Thigh} = 0.843$ kg; $m_{Shank} = 0.804$ kg; $m_{Foot} = 0.342$ kg
Total mass	$\sim 9.2$ kg (the CoM is located at $\sim 0.14$ m above the hip joint )

dynamics model contains the rigid whole-body structure and the actuation dynamics. These two levels are consistently connected by the corresponding transmitted torques. Additionally, a detailed ground contact model considering collision, friction and stiction force is included to simulate realistic ground reaction forces with high time-resolution within reasonable computational time [23]. The rigid body dynamics of the robot consists of a torso and two 3-joint-link serial chains representing the legs that are attached to the torso. The simulation of the generated SimMechanics model is performed by means of a single numerical solver provided by Simulink, without model switching to enable the analysis of impact peak forces and the simulation of flight phases. For the main kinematics and dynamics data of the rigid skeleton we refer to Table I. The highly complex dynamics models of the active and passive monoarticular tendons were derived from the classical mechanical principle of virtual displacement and work to determine the motor and joint torques, the nonlinearly changing lever arms and transmission stiffnesses of the tendons [17]. All models including the full MBS dynamics model and the realistic ground contact model were experimentally validated and shown to match the behavior of the real robot.

### B. Control Approaches

The controller performs different tasks to the joints' actuators during stance and flight. According to human hopping in place, the main source of energy injection is the ankle joint, and knee and hip joints do not move considerably [24]. Thus, the duty of knee and hip joints is setting the joints' angles to adjust the leg during flight phase and tracking the desired configuration during stance.

1) *Bouncing via approximated VMC*: By simplification of the robot model with segmented leg to the SLIP model, we try to produce similar leg behavior during stance phase. Defining a virtual leg from hip to foot tip, the leg motion can be described by its angle and length (see Fig. 2). In SLIP model, the leg force is produced by  $F_s = k_s(l - l_0)$ , in which  $k_s$ ,  $l$  and  $l_0$  are the leg stiffness, length and rest length, respectively.

Suppose that the angle between the foot and the virtual leg direction remains about constant<sup>3</sup>. Then, in order to

produce leg force similar to SLIP ankle torque needs to be proportional to  $F_s$  during the stance phase  $\tau = k(l - l_0)$ , where  $k$ ,  $l$  and  $l_0$  are the stiffness, leg length and rest length of the virtual leg. With this ankle torque, an approximation of the Virtual Model Controller is realized which turns the leg model close to SLIP. The virtual leg length  $l$  is estimated using the joint angles.

In the real robot, damping exists which should be compensated during stance phase. In our controller, the virtual leg rest length and stiffness are changed at mid-stance moment. With this technique, the leg force (respectively, ankle joint torque) remains continuous, while the stored energy increases. In the E-SLIP model [25], it was shown that to add a specific amount of energy  $\Delta E$  at mid stance moment, stiffness and rest length should change as follows:

$$l_0^{new} = \frac{2\Delta E}{k^{old}(l - l_0^{old})} \quad (1)$$

$$k^{new} = \frac{k^{old}(l - l_0^{old})}{(l - l_0^{new})} \quad (2)$$

With these new values, the energy losses are compensated and stable motion can be generated. Without energy compensation, the system will loose energy and fall. Although the amount of lost energy is not known, with this energy compensation approach, it converges to a new equilibrium point. The initial value of leg rest length is computed by the virtual leg length with desired leg configuration, at the first touch down moment. For leg stiffness, the initial value  $k_0$  is set by the designer. We consider a range adopted from human leg stiffness [26] which is scaled by weight ratio of human to robot and results in  $500 < k_0 < 3500$ .

2) *Leg adjustment during the swing phase*: As mentioned before, in [11] a new leg placement strategy was presented as the a robust and stable approach for hopping and running motions with the SLIP model. In this approach the angle between the CoM velocity and the gravity vectors are employed to determine the desired leg angle. Hence, increasing the CoM velocity without changing the direction of this vector never changes the desired leg angle which is the main drawback of this method. In [12], to solve this problem, a modified version of this strategy was introduced as:

$$\begin{aligned} \vec{V} &= [v_x, v_y]^T ; \vec{G} = [0, -g]^T \\ \vec{O} &= \mu \vec{V} + (1 - \mu) \vec{G} \end{aligned} \quad (3)$$

<sup>3</sup>This assumption is verified later in the results and the angles' definitions are explained more in Sec.II-B.2.

in which the leg direction is given by vector  $\vec{O}$ , a weighted average of the CoM velocity vector  $\vec{V}$  and the gravity vector  $\vec{G}$  (See Fig. 3(a)). The weight of each vector is determined by coefficient  $0 < \mu < 1$ . When  $\mu = 1$ , the leg is parallel to the CoM velocity vector and, for  $\mu = 0$ , the leg is exactly vertical. In the rest of the paper, we will refer to this strategy as the Velocity-Based Leg Adjustment VBLA. Unlike Peuker's approach which considers the angle of velocity vector, in VBLA, using both magnitude and angle of the velocity vector increase the robustness of the method against high perturbations.

The advantages of the new method are shown for running and hopping with SLIP model [27]. Its similarity to human hopping strategy in coping with perturbation was shown in [28]. With this approach, running in a large range of velocities can be obtained.

During flight phase, the desired knee and ankle angles are set to fixed values which are determined beforehand. The leg angle ( $\alpha$ ) is obtained by  $\alpha' + \delta$  as shown in Fig. 3(b). Since during motion  $\delta$  does not considerably change, this is approximated by the following equation.

$$\bar{\alpha} = \varphi_1 + \frac{\varphi_2}{2} + \delta_0 \quad (4)$$

Here,  $\delta_0$  is a fixed value to approximate  $\delta$  in Fig. 3(b) which is set to  $10^\circ$  in the rest of this paper and the remaining part equals to  $\alpha'$ . Therefore, the leg angle is adjusted using hip actuator. At each instance, the desired leg angle is computed via Eq. (3) and by measuring knee angle  $\varphi_2$ , the desired hip angle ( $\varphi_h$ ) is given by

$$\varphi_h = \tan^{-1}\left(\frac{O_y}{O_x}\right) - \frac{\varphi_2}{2}. \quad (5)$$

Finally, other target angles are set to fixed values and position control is obtained using PD controllers.

3) *Balancing, locomotion with upright trunk*: Upright upper body is a crucial aspect of human/animal locomotion [16]. Balancing the trunk is an important elementary task in legged locomotion. In this paper, due to design limitations of the robot the trunk is kept upright via a constraining mechanism. This is because of low inertial (short distance between hip and trunk CoM) of the trunk with respect to the legs. This will be resolved in the next generation of BioBiped robot. However, in the rest of the paper, we consider upright trunk, which is satisfied by physical constraints. Therefore the trunk can move in sagittal plane, but cannot rotate. This is in the same direction with our hopping experiments on a fixed or moving treadmill with BioBiped robot whose trunk

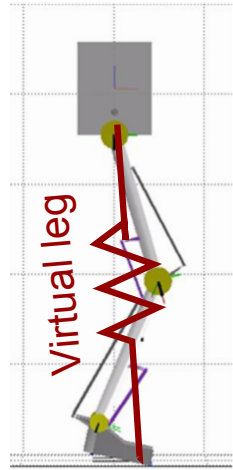


Fig. 2. The musculoskeletal leg is represented by a virtual leg from hip to foot tip.

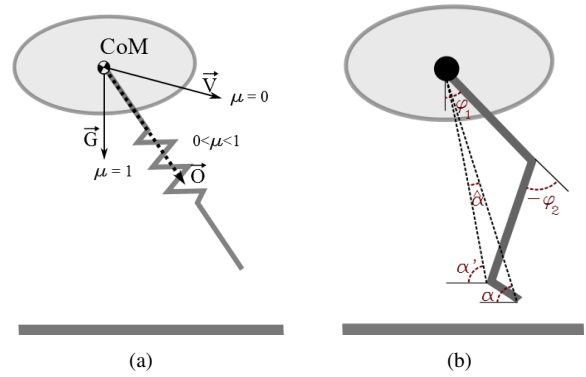


Fig. 3. (a) Velocity Based Leg Adjustment. (b) Virtual leg angle estimation in 3-segmented leg.

is constrained with a frame preventing rotation<sup>4</sup>. This is the intermediate step to do freely hopping on treadmill.

### C. Human Hopping Experiment

Since BioBiped is a bio-inspired robot, comparison with human hopping is helpful to improve the future generations of this robot and also can show how close we are in design and control to produce gaits compared to humans' gaits. We have done hopping experiments with 6 different subjects with body masses between 61 kg and 84 kg and heights between 1.60 m and 1.85 m. The task was hopping in place and kinematic data and force data were measured by a Qualisys motion capture system and a Kistler force plate, respectively. Each experiment takes 30 seconds, starting with 5 seconds standing, 20 seconds hopping and finishing with 5 seconds standing. With the kinematic data we estimated leg angle and leg length from 5<sup>th</sup> metatarsal joint (the joint at the smallest toe) and trochanter (hip point) markers. Center of mass is also estimated by integrating twice ground reaction forces with initial position and velocity of sacrum [29].

## III. RESULTS

With the controller presented in the previous section, not only hopping in place and forward bipedal hopping can be produced, but also switching from one task to another is possible. With respect to specific initial conditions, Changing  $\mu$ , virtual leg stiffness and injected energy  $\Delta E$  result in different gaits. The simulation starts from apex point in which the robot falls down with zero vertical velocity and the initial conditions include leg desired configuration, initial hopping height and horizontal velocity.

In the first experiment, the motion starts with zero horizontal velocity, hopping height equal to 20 cm,  $\mu = 0.82$ ,  $k_0 = 2000 \text{ N/m}$  and  $\Delta E = 5 \text{ J}$ . Stable hopping in place is achieved as it is shown in Fig. 4. In this motion, the CoM speed is slightly larger than zero during flight phase which is compensated by a sharp negative peak in stance phase. It is qualitatively similar to human hopping, shown

<sup>4</sup>See <http://www.biobiped.de> for some videos showing the experimental setup. The control approach in the experiments is different from the proposed approach in this paper.

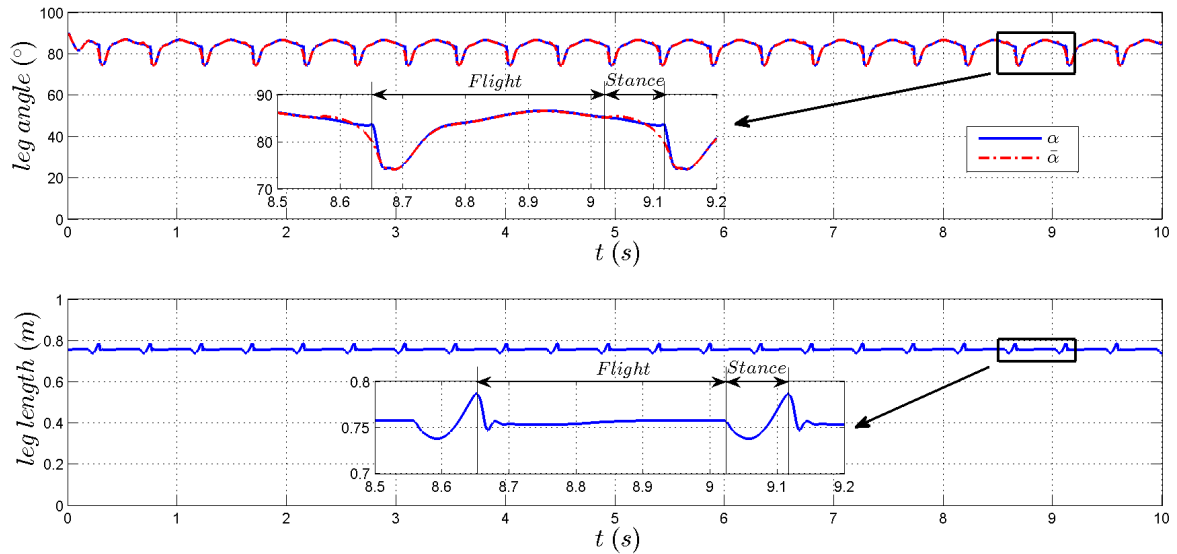


Fig. 7. Leg angle and leg lengths for hopping in place of BioBiped robot. Approximation of leg angle which is used for leg adjustment is also shown in top figure.

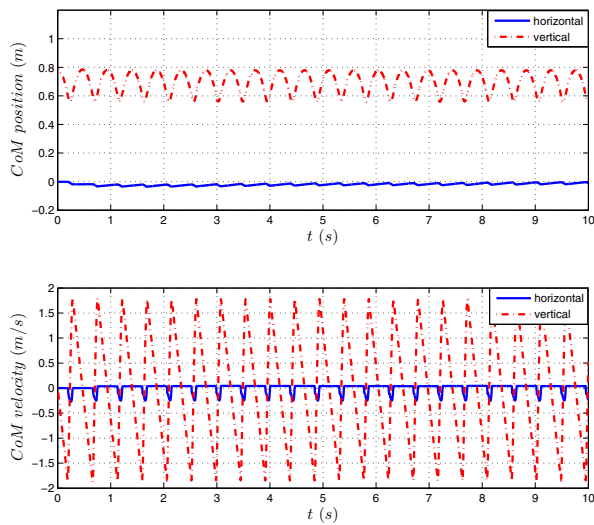


Fig. 4. CoM position and velocity for hopping in place with BioBiped.

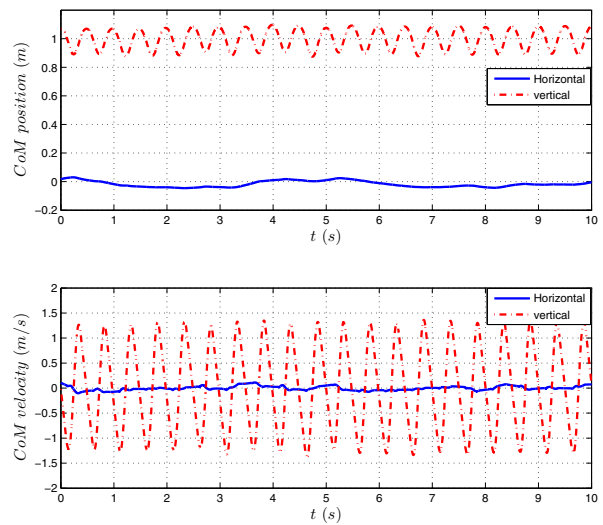


Fig. 5. CoM position and velocity for hopping in place of human.

in Fig. 5. The vertical displacement and speed are very similar. In human hopping in place, the horizontal speed is not exactly zero and it might be positive or negative and if the subject hops with closed eyes, he/she cannot keep the hopping point. This phenomena can be seen in Fig. 6, where the CoM position changes during time with different manners for different subjects. The results are comparable to what obtained with BioBiped, in which at each moment reduction in magnitude of CoM speed is important, not returning to the starting position. Different patterns for hopping in place can be produced by changing the aforementioned parameters  $\mu$ ,  $k_0$  and  $\Delta E$  (see Fig. 6).

In Fig. 7, the leg angle and length are drawn during the gait. The approximation of the leg angle ( $\hat{\alpha}$ ) is very close to the real value. It means that  $\delta$  in Fig. 3(b) is almost constant. The same accuracy is observed in all other experiments too. In both human and BioBiped hopping in place, the leg angle starts to decrease after take off and increase to values close to the beginning of the flight phase before touch down. In robot motion the variation is more than it for human hopping. In the stance phase small changes observed in leg angle from beginning to end. In contrary to human motion, the stance phase is shorter in BioBiped hopping.

Considering different leg lengths of human and robot,

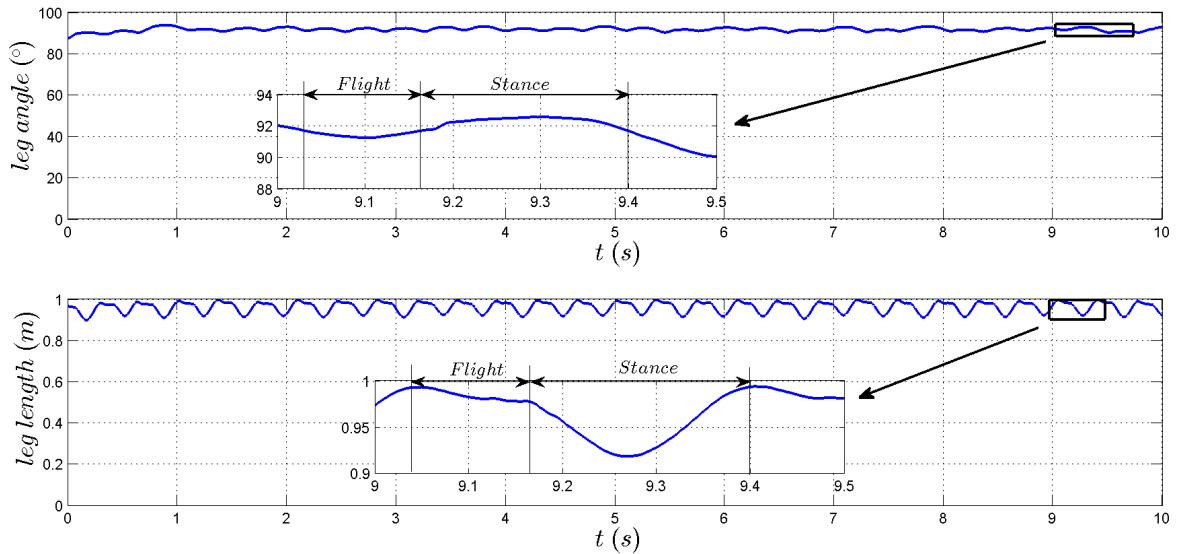


Fig. 8. A sample of human leg kinematics in hopping.

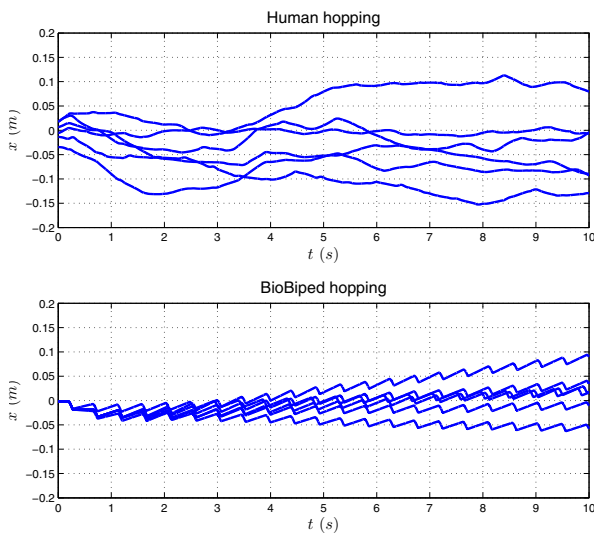


Fig. 6. CoM horizontal motion comparison between human and BioBiped. The robot motion patterns change with changing control parameters  $\mu$ ,  $k_0$  and  $\Delta E$ .

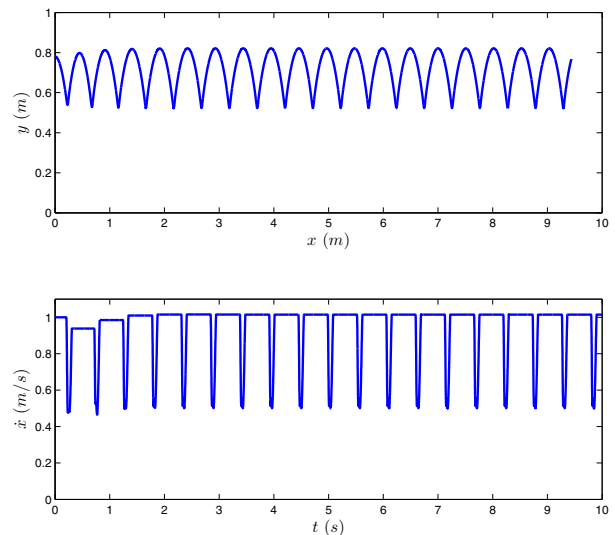


Fig. 9. CoM position and velocity in forward hopping of BioBiped.

comparison of the leg length patterns show that they are similar in stance phase. Higher leg length at take off than at touch down shows increasing the leg rest length during stance phase as in [25]. In flight phase, decreasing the length occurs in both cases, with different strategies. In human gait, it shortens moderately, but in robot motion it starts with a sharp drop and then increasing smoothly.

In the next experiment, forward hopping with different horizontal speeds are achieved. Again finding the correct combination of control parameters is the key to reach the desired speed. This makes a trade off between braking with leg adjustment and thrusting via ankle energy injection

approach. Fig. 9 shows the results for hopping with  $1 \text{ m/s}$ . This illustrates the ability of regulating the horizontal speed to a fixed value.

In the last experiment, the robot falls with zero velocity; by adjusting the parameters  $\mu = 0.9$ ,  $\Delta E = 20$  and  $k_0 = 3000$  switching from hopping in place to forward hopping occurs (See Fig. 10). After 10 seconds, reducing leg adjustment coefficient and injected energy to  $\mu = 0.75$  and  $\Delta E = 1$  results in decreasing system energy and more vertical leg which are needed for hopping with zero speed. The CoM horizontal speed and position illustrate this switching gait. Lower hopping height in the beginning and end of motion shows the lower energy of the system which resulted from



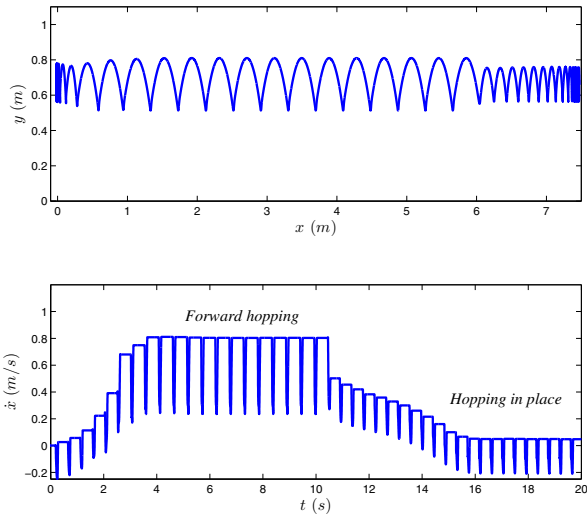


Fig. 10. CoM motion and velocity of switching between hopping in place and forward hopping with BioBiped.

smaller  $\Delta E$  and more vertical leg orientation.

#### IV. DISCUSSION

SLIP model based ankle joint torque control with changing stiffness and spring rest length to manage the energy of the system is employed for stance phase of hopping of BioBiped robot. The VBLA is utilized for leg adjustment in flight phase to tune the motion velocity and perturbation attenuation. The other angles are set to predefined values. With this control approach robust hopping is obtained and different speeds can be attained just with tuning the parameters.

With such a simple controller, a set of two leg motions<sup>5</sup> is provided to the BioBiped as a bioinspired robot. Note that the upright trunk configuration is provided by physical constraints (frame). Similarity between human and robot hopping in place is illustrated in the first part of the results. Without visual feedback, zero velocity is not possible for human. Even with open eyes, more than 15 centimeters horizontal deviation from starting point were observed in 10 seconds of the presented experiments. Since the subjects are asked to hop with their preferred height and frequency, different gaits patterns are observed. Changing the gait patterns is easily achieved with varying parameters of the robot controller. It can be concluded that the required information for human hopping is absolutely low. Injecting a fixed amount of energy corresponding to the hopping height and a mechanism to adjust the leg with respect to velocity vector which can be prepared by a mechanical structure are the two basic requirements. In this study, the energy is just added by ankle joint as a push off force, but the knee and even the hip joint can also contribute to distribute the required torque during stance phase. It might yield other hopping patterns changing the stance and flight duration.

<sup>5</sup>Moving two legs for forward hopping or hopping in place.

The leg behavior including length and angle changes are qualitatively similar between humans and the model predictions. With the stiff leg, considered in Fig. 7, stance phase is shorter than the swing phase. This ratio may be other way around when the leg spring is sufficiently soft. Flight phase duration is mostly related to the hopping height tuned by the injected energy. Therefore, by adjusting the virtual leg stiffness and injected energy, hopping with shorter flight phase and longer stance phase can be achieved. The ration between duration of stance and flight phases is also different depending on the selected human gait, even if they hop with the same frequencies. It depends mostly on how much knee and ankle joints are used to store and return the energy.

The second achievement was producing forward hopping with a constant speed. The results show that if the initial speed is close to the desired ones, sufficient push off ankle torque and appropriate leg angle are provided. This means that the controller requires a proper mapping between the coefficients and desired motion. Then, for faster motion, first required to produce sufficient forward speed. Then, by tuning the parameters the new speed can be realized. In other words, changing the fixed point and moving the states inside the basin of attraction of new fixed point can change the gait speed. This approach simplifies the control and the speed when is automatically realized by a correct set of parameters.

Finally, switching between different gait speeds is accomplished based on the aforementioned scheme. Here, we showed that when the states are in the region of attraction of two different fixed points with different parameters and desired speeds, changing the parameters is enough to change the speed. Hence, with changing the parameters you differ the equilibrium solution (it is a limit cycle, which can be represented as a fixed point by using a Poincaré section) from one to another and since the states of the system are placed in the region of attraction of both fixed points, it can easily switch between them by parameter adjustment.

As the next step we aim at implementing the proposed approach to make a stable running or one leg hopping. Trunk stabilization could be achieved with approaches like Virtual Pendulum Posture control (VPPC) in which the torques are produced such that the ground reaction forces are redirected toward the virtual pivot point (VPP) [16]. This strategy is similar to human and animal locomotion and could be employed for trunk stabilization during stance phase.

#### REFERENCES

- [1] R. Blickhan, "The spring-mass model for running and hopping," *Journal of Biomechanics*, vol. 22, no. 11, pp. 1217–1227, 1989.
- [2] A. Seyfarth, H. Geyer, M. Guenther, and R. Blickhan, "A movement criterion for running," *Journal of Biomechanics*, vol. 35, no. 5, pp. 649–655, 2002.
- [3] H. Geyer, A. Seyfarth, and R. Blickhan, "Compliant leg behaviour explains basic dynamics of walking and running," *Proceedings of the Royal Society B*, vol. 273, no. 1603, pp. 2861–2867, 2006.
- [4] R. J. Full and D. Koditschek, "Templates and anchors: Neuromechanical hypotheses of legged locomotion on land," *Journal of Experimental Biology*, vol. 22, pp. 3325–3332, 1999.
- [5] M. H. Raibert, *Legged Robots that Balance*. MIT Press, Cambridge MA, 1986.

- [6] U. Saranlı, M. Buehler, and D. Koditschek, "Rhex: a simple and highly mobile robot," *International Journal of Robotic Research*, vol. 20, no. 7, pp. 616–631, 2001.
- [7] J. Pratt, "Exploiting inherent robustness and natural dynamics in the control of bipedal walking robots," Ph.D. dissertation, Massachusetts Institute of Technology, 2000.
- [8] J. E. Pratt, C. M. Chew, A. Torres, P. Dilworth, and G. Pratt, "Virtual model control: An intuitive approach for bipedal locomotion," *International Journal of Robotics Research*, vol. 20, no. 2, pp. 129–143, 2001.
- [9] A. Sato and M. Buehler, "A planar hopping robot with one actuator: Design, simulation, and experimental results," in *4 IEEE/RSJ International Conference on Intelligent Robots and Systems*, 2004.
- [10] I. Poulakakis and J. W. Grizzle, "The spring loaded inverted pendulum as the hybrid zero dynamics of an asymmetric hopper," *IEEE Transactions on Automatic Control*, vol. 54, no. 8, pp. 1779–1793, 2009.
- [11] F. Peuker, C. Maufroy, and A. Seyfarth, "Leg adjustment strategies for stable running in three dimensions," *Bioinspiration and Biomimetics*, vol. 7, no. 3, 2012.
- [12] M. A. Sharbafi, C. Maufroy, A. Seyfarth, M. J. Yazdanpanah, and M. N. Ahmadabadi, "Controllers for robust hopping with upright trunk based on the virtual pendulum concept," in *IEEE/RSJ International Conference on Intelligent Robots and Systems (IROS 2012)*, 2012.
- [13] A. D. Kuo, "Energetics of actively powered locomotion using the simplest walking model," *Journal of Biomechanical Engineering*, vol. 124, pp. 113–120, 2002.
- [14] D. G. E. Hobbelen and M. Wisse, "A disturbance rejection measure for limit cycle walkers: The gait sensitivity norm," *IEEE Transactions on Robotics*, vol. 23, no. 6, pp. 1213–1224, 2007.
- [15] A. D. Kuo, "The six determinants of gait and the inverted pendulum analogy: A dynamic walking perspective," *Human Movement Science*, vol. 26, no. 4, pp. 617–656, 2007.
- [16] H. M. Maus, S. Lipfert, M. Gross, J. Rummel, and A. Seyfarth, "Upright human gait did not provide a major mechanical challenge for our ancestors," *Nature Communications*, vol. 1, no. 6, pp. 1–6, 2010.
- [17] K. Radkhah, T. Lens, and O. von Stryk, "Detailed dynamics modeling of BioBiped's monoarticular and biarticular tendon-driven actuation system," in *IEEE/RSJ International Conference on Intelligent Robots and Systems (IROS)*, October 7 - 12 2012, pp. 4243 – 4250.
- [18] K. Radkhah, "Advancing musculoskeletal robot design for dynamic and energy-efficient bipedal locomotion," Ph.D. dissertation, Technische Universität Darmstadt, 2013.
- [19] K. Radkhah, C. Maufroy, M. Maus, D. Scholz, A. Seyfarth, and O. von Stryk, "Concept and design of the BioBiped1 robot for human-like walking and running," *International Journal of Humanoid Robotics*, vol. 8, no. 3, pp. 439–458, 2011. [Online]. Available: <http://www.worldscinet.com/ijhr/08/0803/S0219843611002587.html>
- [20] L. Grègoire, H. E. Veeger, P. A. Huijing, and G. J. van Ingen Schenau, "Role of mono- and biarticular muscles in explosive movements," *International Journal of Sports Medicine*, vol. 5, pp. 301–305, 1984.
- [21] R. Jacobs, M. F. Bobbert, and G. J. van Ingen Schenau, "Mechanical output from individual muscles during explosive leg extensions: The role of biarticular muscles," *Journal of Biomechanics*, vol. 29, no. 4, pp. 513–523, April 1996.
- [22] K. Radkhah and O. von Stryk, "Actuation requirements for hopping and running of the musculoskeletal robot BioBiped1," in *IEEE/RSJ International Conference on Intelligent Robots and Systems (IROS)*, September 25 - 30 2011, pp. 4811–4818.
- [23] T. Lens, K. Radkhah, and O. von Stryk, "Simulation of dynamics and realistic contact forces for manipulators and legged robots with high joint elasticity," in *International Conference on Advanced Robotics (ICAR)*, June 20-23 2011, pp. 34–41.
- [24] S. W. Lipfert., *Kinematic and dynamic similarities between walking and running*. Verlag Dr. Kovač., 2010.
- [25] C. Ludwig, S. Grimmer, A. Seyfarth, and H. Maus, "Multiple-step model-experiment matching allows precise definition of dynamical leg parameters in human running," *Journal of Biomechanics*, vol. 45, no. 14, pp. 2472–5, 2012.
- [26] C. Farley and D. Morgenroth, "Leg stiffness primarily depends on ankle stiffness during human hopping," *Journal of Biomechanics*, vol. 32, pp. 267–273, 1999.
- [27] M. A. Sharbafi, M. N. Ahmadabadi, M. J. Yazdanpanah, and A. Seyfarth, "Novel leg adjustment approach for hopping and running," in *Dynamic Walking*, 2013.
- [28] M. A. Sharbafi and A. Seyfarth, "Human leg adjustment in perturbed hopping," in *AMAM*, 2013.
- [29] S. A. Gard, S. C. Miff, and A. D. Kuo, "Comparison of kinematic and kinetic methods for computing the vertical motion of the body center of mass during walking," *Human Movement Science*, vol. 22, pp. 597–610, 2004.